FORSCHUNGSZENTRUM ROSSENDORF

Mitglied der Wissenschaftsgemeinschaft Gottfried Wilhelm Leibniz

WISSENSCHAFTLICH-TECHNISCHE BERICHTE

FZR-339

Januar 2002

ISSN 1437-322X

Roland Kotte and Burkhard Kämpfer

Acceptance and count rate estimates for experiments on subthreshold Phi meson production in central collisions of C+C at 2 A·GeV

Herausgeber:
Forschungszentrum Rossendorf e.V.
Postfach 51 01 19
D-01314 Dresden
Telefon +49 351 26 00
Telefax +49 351 2 69 04 61
http://www.fz-rossendorf.de/

Als Manuskript gedruckt

FORSCHUNGSZENTRUM ROSSENDORF

WISSENSCHAFTLICH-TECHNISCHE BERICHTE

FZR-339

Januar 2002

Roland Kotte and Burkhard Kämpfer

Acceptance and count rate estimates for experiments on subthreshold Phi meson production in central collisions of C+C at 2 A·GeV

Acceptance and count rate estimates for experiments on subthreshold Phi meson production in central collisions of C + C at 2 A·GeV

R. KOTTE AND B. KÄMPFER
Forschungszentrum Rossendorf, PF 510119, 01314 Dresden, Germany
(January 14, 2002)

Monte-Carlo estimates of the subthreshold ϕ meson production are performed for the reaction $^{12}C + ^{12}C$ at 2 A·GeV assuming the ϕ's to be emitted isotropically and distributed thermally in the center-of-mass system of the colliding nuclei. Different scenarios involving the detector installations FOPI and HADES at SIS/GSI are considered to determine the expected yields of $\phi(1020)$ mesons identified via the K^+K^- and e^+e^- decay channels.

I. INTRODUCTION

In the past years, the study of in-medium properties of hadrons produced in heavy-ion collisions (HIC) has attracted increasing interest. Since subthreshold particle production has been found sensitive to medium modifications of hadron properties [1–4], substantial effort has been made in the beam energy region 1 - 2 A·GeV covered by the heavy-ion synchrotron SIS at GSI Darmstadt. Especially, the recently measured observables like antikaon production cross sections, phase-space distributions and K^+/K^- ratios [5–11] are discussed extensively whether they provide hints to a possible reduction of the antikaon mass in dense nuclear matter [4,12–21].

To be able to compare quantitatively the experimental data on antikaon production with the output of transport approaches, all relevant elementary hadronic processes should be modelled reliably. A quite important intermediate state seems to be the production of the vector meson $\phi(1020)$ which decays with a branching ratio of 49.2 % into a pair of charged kaons. In contrast to the quite sizeable amount of experimental data for open strangeness production in HIC at SIS energies, analogous data on mesons with hidden strangeness, i.e. the ϕ, is rather scarce [22,23]. Moreover, also few information is available from theory concerning the different ϕ producing elementary channels. There are a few groups working on this topic [25–33]. Here, measurements of the cross sections of elementary ϕ processes, like the reaction $pp \to pp\phi$ recently investigated by the DISTO collaboration [34] at an excess energy of $\sqrt{s} - \sqrt{s_{thr}} = 83$ MeV, are extremely helpful for adjusting the model parameters; further data at 18.5 MeV and 34.6 MeV are to be expected from ANKE [35]. However, similar data are necessary also for other channels, especially near to the corresponding production thresholds. There, the models are most sensitive. In ref. [32] the role of three-body collisions for ϕ production was studied. It turned out that they can be well described by consecutive two-body processes inside the nuclear medium. In ref. [33] new elementary processes were included in the BUU type transport code used to calculate the ϕ production. Especially, the channels $\rho N \to \phi N$ and $\rho\Delta \to \phi N$ were found to increase the number of ϕ's substantially in comparison to those calculations which did not include these channels [27,36].

The behaviour of the ϕ meson within a nuclear environment has been investigated, too. The shift of the mass peak is expected to be small [3,37]. However, the width could

be changed drastically. Thus, at normal nuclear matter density, $\rho = \rho_0$, the authors of refs. [37] and [38] predict an increase of the width by factors of 10 and 5, respectively. This decreases the life time drastically and a substantial part of the ϕ's should decay within the collision zone of a heavy-ion reaction. However, the daughter kaons would be also subjected to the influence of the nuclear medium. Thus, in order to attack such questions, like in-medium modifications of vector mesons, with an undisturbed probe, the investigation of the leptonic decay $\phi \rightarrow e^+e^-$ is more appropriate. Corresponding measurements are planned with the dilepton spectrometer HADES [39] currently put into operation at SIS/GSI.

It is the aim of the present paper to discuss the feasibilities of future dedicated studies of ϕ meson subthreshold production in heavy-ion collisions. To have a benchmark-like estimate of expected maximum count rates, we report here on Monte-Carlo simulations for the detection of the ϕ's produced in central reactions of C + C at 2 A·GeV involving both the hadronic ($\phi \rightarrow \mathrm{K^+K^-}$) and the leptonic ($\phi \rightarrow \mathrm{e^+e^-}$) decay channels. In subsequent simulations the background must be accounted for; this is relegated to future work.

Our paper is organized as follows. In the next section, references to the experimental details of the detectors are given. In section III, the simulation procedure is described. In section IV, yields of ϕ mesons are estimated for two different detector setups, i.e. FOPI and HADES, involving various phase-space regions. Finally, the paper concludes with a summary in section V.

II. EXPERIMENTS

The envisaged experiments can be performed at the SchwerIonenSynchrotron SIS at GSI Darmstadt. Carbon (graphite) targets of ~ 1 mm thickness (i.e. about 1% interaction probability) have to be irradiated by ^{12}C ions of 2 A·GeV beam energy, the highest one available for light ions. The charged particles produced in this reaction including the decay products of short living resonances like the vector meson $\phi(1020)$ can be measured either with the 4π detector FOPI or with the High-Acceptance Di-Electron Spectrometer HADES. Both installations allow for almost full angular coverage in azimuthal direction. Details of the present and upgraded versions of the FOPI setup can be found in refs. [40,41] whereas the HADES spectrometer is described in ref. [39]. Notice, detailed information on both detectors/experiments are provided on the corresponding web sites http://www-aix.gsi.de/~fopiwww/ and http://www-hades.gsi.de/.

III. SIMULATION

In order to get a statistically significant measure of the detector acceptance for correlated $\mathrm{K^+K^-}$ emission, Monte Carlo simulations have been performed (10^6 events for each parameter set). In these simulations, the ϕ's are modelled by an initial mass distribution of Breit-Wigner shape with the mean mass $m_\phi = 1019.4$ MeV and the width $\Gamma_\phi = 4.4$ MeV [42]. They are emitted isotropically in the c.m. system of the colliding nuclei according to simulations [36] with the IQMD approach [43]. The expanding thermal source is characterized by two parameters, the temperature T and the radial flow velocity β_r, as proposed by Siemens and Rasmussen for an expanding spherical shell [44]. In contrast to intermediate mass fragments produced in a central heavy-ion collision which are particularly sensitive to collective motion effects [45] the effect of the radial flow is small

for light particles, e.g. protons or ϕ mesons. Thus, both parameters can be combined to an effective temperature T_{eff}[1]. It appears as inverse slope parameter of the transverse mass ($m_t = \sqrt{p_t^2 + m_\phi^2}$) distribution

$$\frac{1}{m_t^2 cosh(y')} \frac{d^2N}{dy' dm_t} = N \cdot \exp\left(-\frac{m_t \cdot cosh(y')}{T_{eff}}\right) \quad (1)$$

at midrapidity $y' = y - y_{cm} = 0$. In the following we use this effective inverse slope parameter, i.e. $T_\phi = T_{eff}$, when simulating the ϕ phase-space distributions[2].

In case of the decay channel $\phi \rightarrow K^+K^-$, only those pairs, where both the kaon and the antikaon survive the decay in flight on the way to the time-of-flight (TOF) detectors, are detected within the corresponding phase space regions. To account for the kaon decay in HADES a constant flight path from the target to the TOF detectors of 210 cm is assumed. For the FOPI detector combination of the Central Drift Chamber plus the TOF Barrel (CDC/Bar) a constant transverse distance from the target to the barrel of 111 cm is implemented. For the FOPI detectors Helitron plus Plastic Wall (Hel/Pla) the flight path (in cm) to the scintillator strips is parametrized as function of the polar angle (in degrees), i.e. $l_{TOF} = 525 - 9.2 \cdot \theta$ for $7^o < \theta < 12.5^o$ and $l_{TOF} = 443 - 2.6 \cdot \theta$ for $12.5^o < \theta < 30^o$.

In order to simulate the finite velocity resolution the kaon TOF is smeared out by a dispersion of $\sigma_{TOF} = 200$ ps used for both detector setups. For the leptonic decay $\phi \rightarrow e^+e^-$ to be studied with HADES a constant relative momentum resolution of $\delta p/p = 0.015$ is assumed.

IV. BEAM TIME ESTIMATES

A. The decay channel $\phi \rightarrow e^+e^-$ to be measured with HADES

The expected ϕ rate from the reaction C (2 A·GeV) + C → X + ϕ → X + e^+e^- is calculated via the relation

$$\dot{N}_{\phi \rightarrow e^+e^-} = \dot{N}_b \cdot \left(\frac{\dot{N}_{tot}^{reac}}{\dot{N}_b}\right) \cdot \epsilon_{DA} \cdot \left(\frac{\sigma_\phi}{\sigma_{K^-}}\right) \cdot \left(\frac{\sigma_{K^-}}{\sigma_{tot}}\right) \cdot \epsilon_{det} \cdot \epsilon_{trig} \cdot \epsilon_{acc}^{\phi}(T_\phi, \Delta\theta_e, \Delta p_e). \quad (2)$$

Here, we abbreviate:

- average beam intensity $\dot{N}_b = 5 \cdot 10^7$/s (i.e. 10^8/s at 50 % duty cycle),
- target thickness $\frac{\dot{N}_{tot}^{reac}}{\dot{N}_b} = 1$ % interaction length,

---

[1]Indeed, no significant difference has been observed for the ϕ phase-space distributions generated with simulations using either both the T and β_r parameters or those using only T_{eff} while keeping $\beta_r = 0$.

[2]Usually, the experimental m_t spectra are generated for a set of rapidity slices according to eq. (1). With the assumption of a single exponential slope each spectrum can be extented into the unmeasured regions and then integrated to get the corresponding absolute yield at a certain value of rapidity [46,47].

- data acquisition dead time factor $\epsilon_{DA} = 50\,\%$,
- triggers
  - 1^{st} level (central, high charged-particle multiplicities): minimum bias/central suppression of 1/3 only (for small systems like C+C not very efficient),
  - 2^{nd} level (online lepton ID): 1 % of total cross section;

  these allow a taping rate of $2.5 \cdot 10^3$ events/s corresponding to a total of $2.2 \cdot 10^8$ 2^{nd} level trigger events per day,
- ϕ/K^- ratio $\frac{\sigma_\phi}{\sigma_{K^-}} \simeq 0.2$ (taken from Au (10.8 A·GeV)+ Au collisions at AGS energies [48,49]; this value changes with beam energy [50]; preliminary experimental values for Ru (1.69 A·GeV)+ Ru and Ni (1.93 A·GeV)+ Ni are larger [23,24]),
- antikaon multiplicity $\frac{\sigma_{K^-}}{\sigma_{tot}} = 2 \cdot 10^{-4}$ (measured by KaoS for C (2.0 A·GeV) + C collisions [7]),
- total $\mathrm{e}^+\mathrm{e}^-$ pair detection efficiency $\epsilon_{det} = 0.7^2 \cdot 0.95^2 \cdot 0.8^2 \cdot 0.85^2 = 0.2$; i.e. average single electron detection efficiencies in RICH (70 %) + MDC (95 %) + META (80 %) and dead zone effects (-15 %),
- 2^{nd} lvl. trigger efficiency $\epsilon_{trig} = 0.9$,
- acceptance factor $\epsilon^{\phi}_{acc} = \epsilon^{\phi \to e^+e^-}_{acc}(T_\phi, \Delta\theta_e, \Delta p_e)$ (including the branching ratio $\frac{\Gamma_{\phi \to e^+e^-}}{\Gamma_{\phi,tot}} = 3 \cdot 10^{-4}$) depends on $\mathrm{e}^\pm$ polar angle and momentum regions $\Delta\theta_e$ and Δp_e, respectively; taken from MC simulations which generate the ϕ's by means of the thermal model eq. (1) with inverse slope parameter T_ϕ; full azimuthal coverage is assumed (the shadow effect of the frames of the six sectors the setup is composed of is put into the detection efficiency).

Adopting these values we get

$$\dot{N}_{\phi \to e^+e^-} = 5 \cdot 10^7/s \cdot 0.01 \cdot 0.5 \cdot 0.2 \cdot 2 \cdot 10^{-4} \cdot 0.2 \cdot 0.9 \cdot \epsilon^{\phi}_{acc} = 1.6 \cdot 10^5/d \cdot \epsilon^{\phi}_{acc}. \qquad (3)$$

For instance, for the polar angle range $\Delta\theta_e$ given by $18^o < \theta_e < 88^o$ and an inverse slope parameter of $T_\phi = 70$ MeV we find from figs. 1 and 2 an acceptance factor of $\epsilon^{\phi \to e^+e^-}_{acc} = 1.8 \cdot 10^{-4}$. The acceptance depends only weakly on the inverse slope parameter T_ϕ (cf. full dots in fig. 2), a significant observation since - a priori - one does not know the spectral shape of the ϕ meson. Rather, one has to measure it. With this acceptance eq. (3) yields a rate of 29 ϕ's per day[3].

If, e.g. for reliable particle identification, the lepton momentum range Δp_e has to be restricted to $p_e < 1$ GeV/c the rate would decrease by a factor of two (cf. triangles in fig. 2) thus yielding 14 ϕ's per day only. If the full polar angle range of the META (TOF + Shower) detectors could not be exploited but must be restricted to the TOF acceptance

---

[3]Basically, the difference of our rate and that given in the HADES beam time proposal [51] is due to the difference of the beam intensities and due to the m_t scaling assumed in the proposal yielding a ϕ/K^- ratio of about unity in contrast to our more conservative value of 20 %.

within $44^o < \theta_e < 88^o$ then the acceptance would amount to $2.9 \cdot 10^{-5}$ only (cf. open dots in fig. 2) hence reducing the rate to 5 ϕ's per day.

Finally, without further restrictions the given rate of 28 ϕ's per day would yield a total amount of about 400 ϕ's within a beam time of two weeks. In order to get these rare probes out of the data files one has to calibrate and afterwards to scan about $3 \cdot 9^{10}$ 2^{nd} lvl. trigger events, an amount of data ($\sim$ 20 TByte) requiring sophisticated data processing. Note, without 2^{nd} level trigger the experiment is hardly feasible since the data acquisition is assumed to work already at its upper limit. (The 1^{st} level trigger selecting central collisions via high charged-particle multiplicities is not very efficient in case of small collision systems like ^{12}C+^{12}C.)

B. The decay channel $\phi \rightarrow K^+K^-$ to be measured with HADES

The ϕ rate from the hadronic channel is calculated according to eq. (2) but applying the following changes:

- beam intensity $1.5 \cdot 10^6$/s (to have same taping rate as for dilepton experiment described in section IV A),
- triggers:
  1^{st} level trigger only, assuming a minimum bias/central suppression of 1/3 which allows the same taping rate of $2.5 \cdot 10^3$ events/s as for the leptonic experiment (Sect. IV A),
- total K^+K^- pair detection efficiency (including cut and matching (with TOF detectors) efficiencies and effects of dead zones) $\epsilon_{det} = 0.2$,
- acceptance factor (including the branching ratio $\frac{\Gamma_{\phi \rightarrow K^+K^-}}{\Gamma_{\phi,tot}} = 0.492$) now depends on the $K^{\pm}$ polar angle and momentum regions $\Delta\theta_K$ and Δp_K, respectively, i.e. $\epsilon^{\phi}_{acc} = \epsilon^{\phi \rightarrow K^+K^-}_{acc}(T_\phi, \Delta\theta_K, \Delta p_K)$ (full azimuthal coverage assumed, shadow effects of the sector frames put into detection efficiency).

With these numbers eq. (3) becomes

$$\dot{N}_{\phi \rightarrow K^+K^-} = 1.5 \cdot 10^6/s \cdot 0.01 \cdot 0.5 \cdot 0.2 \cdot 2 \cdot 10^{-4} \cdot 0.2 \cdot \epsilon^{\phi}_{acc} = 5.2 \cdot 10^3/d \cdot \epsilon_{acc}. \qquad (4)$$

From figs. 3 and 4 we find for $T_\phi = 70$ MeV, for the presently available polar angle range of the HADES-TOF detector of $44^o < \theta < 88^o$ and for a maximum kaon momentum of 0.6 GeV/c an acceptance of $6.5 \cdot 10^{-4}$ which increases slightly to $1.0 \cdot 10^{-3}$ if the charged kaons can be identified up to momenta of 1.0 GeV/c. Just like for the FOPI setup (fig. 9), the acceptance factor depends strongly on the inverse slope parameter T_ϕ of the ϕ's generated by the thermal model (cf. fig. 4). Note, there is no acceptance at midrapidity. Consequently, it will be not possible to get a fair reconstruction of the ϕ rapidity distribution by integrating the transverse mass spectra eq. (1) at various rapidity slices. With the given acceptance factor of 0.1%, the rate amounts to 5 ϕ's per day, i.e. significantly less than the yield expected from the upgraded FOPI setup (Sect. IV C 4).

The situation improves dramatically if the HADES-TOF detector could be extended to $18^o < \theta < 88^o$ with high time resolution and sufficient granularity (eventually realized with large area glass resistive plate chambers as planned to be used for the FOPI upgrade

[41]) thus allowing for kaon identification within the full polar angular range covered by the drift chambers [39]. For such an upgraded HADES spectrometer the $\phi \rightarrow K^+K^-$ overall acceptance factor would increase to 3.0 % provided the kaons and antikaons can be identified up to momenta of 1 GeV/c hence allowing an access to the midrapidity region (cf. fig. 5).

We investigated also the effect of a reduced maximum kaon identification momentum (cf. fig. 4). For an upper $K^{\pm}$ momentum of 0.8 GeV/c the acceptance decreases to a value of 2.2 % mostly at the expense of the midrapidity yield (cp. fig. 6). A further reduction of the maximum kaon momentum to 0.6 GeV/c (same figure) would decrease the yield even stronger down to a value of 1.0 % hence loosing almost completely the region around midrapidity where the ϕ yield is expected to be largest. Consequently, future HADES experiments devoted to the hadronic channel $\phi \rightarrow K^+K^-$ should aim at good K^+K^- identification up to momenta of about 1 GeV/c.

Let us compare the ϕ and K^- transverse momentum spectra. Typical midrapidity transverse mass distributions are shown in fig. 7 for transverse kinetic energies up to 0.5 GeV. It is worth mentioning that the $\phi \rightarrow K^+K^-$ decay kinematics leads to slopes of the daughter kaons/antikaons (right panels) being much steeper than those of the mother ϕ's (left panels in fig. 7). Hence, $K^{\pm}$ mesons from the ϕ decay populate mainly the low-energy part of the corresponding spectrum. While for kaons this contribution is small as compared with other, energetically preferred and therefore much stronger, channels like non-resonant, associated strangeness production, it could play an important role for the interpretation of the antikaon spectra. Thus, in case of a sufficiently strong ϕ production, one expects a concave shape of the logarithm of the K^- transverse mass distribution eq. (1). As a result, the assumption of a purely exponential spectrum would make extrapolations into the unmeasured low-energy region of the K^- spectrum rather unreliable. Consequently, one has really to measure this part of the spectrum if one wants to determine the rapidity density distribution and hence the total K^- yield.

Finally, with the given overall acceptance of about 3 % the rate eq. (5) would be by a factor of 30 higher than that estimated for the present HADES setup, i.e. we expect 160 ϕ's per day or $2.2 \cdot 10^3$ after a beam time of two weeks. In order to seek for these rare probes, about $3 \cdot 10^9$ 1^{st} level trigger events, have to be calibrated and scanned. Though this number of events is the same as for the leptonic experiment the total ϕ yield is expected to be an order of magnitude larger than the corresponding estimate of section IV A.

C. The decay channel $\phi \rightarrow K^+K^-$ to be measured with FOPI

The ϕ rate from the hadronic channel to be measured with the upgraded setup [41] of the FOPI detector system [40] is calculated according to eq. (2) but applying the following changes:

- beam intensity $6 \cdot 10^5$/s, (limited by maximum data rate of about 1 kHz central events in case of the collision system C + C),
- triggers:
  1^{st} level (central) trigger only (no dedicated 2^{nd} level (kaon) trigger available yet) demanding a high Pla charged particle multiplicity, minimum bias/central suppression of 1/3, allowing a taping rate of 10^3 event/s,

- acceptance factor (including the branching ratio $\frac{\Gamma_{\phi\to K^+K^-}}{\Gamma_{\phi,tot}} = 0.492$) depends on the $K^{\pm}$ polar angle and momentum (CDC/Bar) or velocity (Hel/Pla) regions allowing kaon detection.

With these numbers eq. (3) becomes

$$\dot{N}_{\phi\to K^+K^-} = 6\cdot 10^5/s \cdot 0.01 \cdot 0.5 \cdot 0.2 \cdot 2 \cdot 10^{-4} \cdot \epsilon_{det} \cdot \epsilon^{\phi}_{acc} = 10.4 \cdot 10^3/d \cdot \epsilon_{det} \cdot \epsilon_{acc}. \quad (5)$$

The K^+K^- pair detection efficiency ϵ_{det}, comprising the $K^{\pm}$ cut and subdetector matching efficiencies, and the ϕ acceptance factors ϵ_{acc} of the different detector combinations are given in the subsequent subsections.

1. Detector combination CDC/Bar

The FOPI detector combination of CDC and upgraded TOF barrel allows kaon identification only for transverse momenta above 0.1 GeV/c which is needed for a particle to reach the barrel[4]. We introduced a similar lower limit in the simulation, for simplicity not to the transverse momentum but to the laboratory momentum. The corresponding $\phi \to K^+K^-$ acceptance difference can be neglected since most of these slow $K^{\pm}$ mesons anyway would decay on the way to the plastic barrel. From fig. 8 we find for $T_\phi = 70$ MeV and a maximum kaon momentum of 0.6 GeV/c an acceptance of $\epsilon_{acc} = 2.9 \cdot 10^{-3}$ which increases to $4.7 \cdot 10^{-3}$ if the charged kaons can be identified up to momenta of 1 GeV/c. Notice the dramatic dependence of the acceptance on the temperature parameter T_ϕ as displayed in fig. 9.

With the given acceptance factor and for a realistic kaon pair detection efficiency of $\epsilon^{CDC/Bar}_{det} = 0.4$, the rate amounts 20 ϕ's per day yielding a total of 280 ϕ's after a beam time of two weeks. This sample is about an order of magnitude larger than previous ϕ yields found for central collisions of Ni(1.93 A·GeV) + Ni [22–24].

2. Detector combination Hel/Pla

Though the mass resolution of the forward FOPI detectors Hel/Pla is not as good as that of CDC/Bar, it allows for the selection of correlated K^+K^- pairs, too. Thus, estimates of ϕ meson yields in the region of highest density, i.e. at low transverse momentum and around midrapidity, can be deduced [23,24]. Assuming a temperature of $T_\phi = 70$ MeV and for the kaon velocity and polar angle ranges of $0.4 < \beta_K < 0.85$ and $15^o < \theta_K < 27^o$, respectively, we find from fig. 10 an acceptance of $4.9 \cdot 10^{-3}$ (lower panels) which increases to $11.1 \cdot 10^{-3}$ if the charged kaons can be measured also for small angles where the Helitron used to exhibit significant efficiency losses. Note, the dependence of the acceptance on the temperature parameter T_ϕ as displayed in fig. 11 is less dramatic than for CDC/Bar.

With the given acceptance factor of about 1.1 % and for a realistic kaon pair detection efficiency of $\epsilon^{Hel/Pla}_{det} = 0.2$, the rate amounts to 23 ϕ's per day yielding a total of 320 ϕ's after a beam time of two weeks.

---

[4]Otherwise, the magnetic field of the solenoid leads to spiral tracks inside the CDC.

3. Mixed detector combination CDC/Bar-Hel/Pla

We estimated also the ϕ acceptance factor if the the K^- mesons will be identified with the CDC/Bar combination of FOPI while the K^+ mesons will be detected within Hel/Pla. The lower left panel of fig. 12 shows the corresponding ϕ distribution in the $p_t - y$ plane. For comparison, the expected ϕ distribution when detecting both kaons and antikaons in CDC/Bar (Hel/Pla) are displayed in the upper left (right) panel. Obviously, the mixed detector combination allows for populating the polar angle region $27^o < \theta < 37^o$ where no decay kaons are detected. The dependence of the acceptance factor on the effective inverse slope parameter T_ϕ is shown in fig. 13 (squares for upgraded, triangles for present FOPI setup). Notice the relative constancy of the acceptance of this particular detector combination over a wide range of slope parameters. With the corresponding acceptance factor (for $T_\phi = 70$ MeV) of $\epsilon_{acc} = 3.7 \cdot 10^{-3}$ and with a combined kaon pair detection efficiency of $\epsilon_{det} = 0.28$ we expect 11 ϕ mesons per day, i.e. 150 ϕ's after a beamtime of two weeks.

4. FOPI total

The lower right panel of fig. 12 shows the overall phase-space coverage when combining the three data sets expected for FOPI subdetectors. Adding the rate expectations of sections IV C 1 to IV C 3, the upgraded FOPI detector system would yield 54 ϕ's per day, i.e. about 750 ϕ mesons after two weeks of beam on target. In order to seek for these rare probes about $1.2 \cdot 10^9$ events have to be calibrated and scanned. This number exceeds previous FOPI event samples by more than two orders of magnitude. However, since the size of a semi-central C+C events is significantly smaller than that of previously processed central Au+Au events, the amount of data is expected to be larger by an order of magnitude only, i.e a few TByte.

V. SUMMARY

In summary, for the collision system C+C at 2 A·GeV we have calculated the ϕ meson acceptance of two large detector setups, the 4π detector FOPI and the dilepton spectrometer HADES at SIS/GSI, which allow to measure either exclusively the decay products of the hadronic channel $\phi \rightarrow K^+K^-$ (FOPI) or both the products of the hadronic and leptonic $\phi \rightarrow e^+e^-$ channels (HADES). We varied the spectral shape of the mother ϕ's and the available phase-space regions in order to be flexible with respect to reliable predictions of both the beam time necessary for a certain ϕ yield and the size of the corresponding event sample which has to be processed.

The largest geometrical acceptance ($\sim 40\,\%$) is achieved with HADES when measuring the $e^\pm$ pairs from the ϕ decay. This channel would allow for the reconstruction of almost the full triple-differential momentum distribution of the ϕ mesons. About 400 ϕ's are expected after a reasonable beam time of two weeks. Note that the assumed beam intensity of $5 \cdot 10^7$/s (on a target of 1 % interaction length) would yield a rather high reaction rate of $5 \cdot 10^5$/s. Presently, it is not proven whether the diamond start detector which is aimed at counting individual beam particles and the various detectors for the reactions products will stand these rates. Anyway, in order to record at a sufficiently low

rate preferentially those events containing lepton candidates a fast and efficient 2^{nd} level trigger is mandatory.

Concerning the hadronic channel, the HADES spectrometer with an upgraded TOF subdetector will provide a geometrical acceptance of 6 % only. But it will still allow for reliable reconstruction of the ϕ distribution and the corresponding total production probability. About 2200 ϕ's are expected within two weeks. In case of the upgraded FOPI setup, the overall geometrical acceptance of all involved subdetector combinations amounts to 4 %. There, about 750 ϕ meson are expected after two weeks of beam on target.

The measurement of the di-kaon decay channel of ϕ mesons produced in heavy ion collisions with the presently available HADES-TOF setup and also with the FOPI setup exploiting only the CDC/Bar detector combination faces the missing acceptance at midrapidity hence making the extrapolation to a 4π multiplicity rather unreliable. The yields expected from two-weeks experiments with these HADES- and FOPI-detector configurations would amount only to 70 and 280 ϕ's, respectively.

As advantage of the di-electron channel we found the weak dependence of the geometrical acceptance on the spectral shape, i.e. the inverse slope parameter T_ϕ, of the mother ϕ's as far as the full momentum range of the $e^\pm$ pairs can be exploited. Even if the $e^\pm$ momenta are restricted to $p_e < 1$ GeV/c the variation of the acceptance is only 30 % over the temperature range of $T_\phi = 60...120$ MeV. For the di-kaon channel this dependence on T_ϕ appears rather strong, especially if the midrapidity kaons are not detected (half to full order of magnitude variation over the relevant range of inverse slope parameters). Note, our usage of an inverse slope of 70 MeV is based on preliminary results [23,24] of subthreshold ϕ meson production in central collisions of Ni + Ni and Ru + Ru. If there would be some deviation from this value the beam time estimates given in section IV can be easily rescaled with the help of the systematics summarized in figs. 2, 4, 9, 11 and 13. The same holds for changes of beam intensity, collision system, detection efficiencies etc.

Some systematic uncertainty of the expected ϕ yield may arise from the assumption of a ϕ/K^- ratio of about 0.2. Since presently for SIS energies the corresponding information is rather scarce this number is taken from Au + Au collisions at 10.8 A·GeV [48,49], i.e. beam energies well above the nucleon-nucleon threshold. Preliminary results on subthreshold ϕ meson production in central collisions of Ni + Ni and Ru + Ru point to even larger values [23,24]. Recent calculations of hadron production in central Au + Au collisions performed with the Giessen HSD approach support this finding [50]. The authors report that the ϕ multiplicity is almost the same at subthreshold energies as the antikaon multiplicity, a finding which still has to be checked experimentally. Thus, the ϕ yields we estimate in the present report might even be larger hence allowing for statistically more significant data samples. The present simulations are aimed at estimating maximum count rates. Background contributions are not yet considered.

---

[1] W. Cassing, V. Meta, U. Mosel and K. Niita, Phys. Rep. **188**, 363 (1990).

[2] U. Mosel, Ann. Rev. Nucl. Part. Sci. **41**, 29 (1991).

[3] T. Hatsuda and S. H. Lee, Phys. Rev. bf C46, R34 (1992); T. Hatsuda, Nucl. Phys. A **544**, 27c (1992); H. Kuwabara and T. Hatsuda, Prog. Theor. Phys. **94**, 1163 (1995).

[4] C. M. Ko and G. Q. Li, J. Phys. G **22**, 1673 (1996).
[5] A. Schröter et al., Z. Phys. A **350**, 101 (1994).
[6] R. Barth et al. (KaoS collaboration), Phys. Rev. Lett. **78**, 4007 (1997).
[7] F. Laue et al. (KaoS collaboration), Phys. Rev. Lett. **82**, 1640 (1999).
[8] P. Senger and H. Ströbele, J. Phys. G **25**, R59 (1999).
[9] F. Laue et al. (KaoS collaboration), Eur. Phys. J. A **9**, 397 (2000).
[10] M. Menzel et al. (KaoS collaboration), Phys. Lett. B **495**, 26 (2000).
[11] K. Wiśniewski et al. (FOPI collaboration), Eur. Phys. J. A **9**, 515 (2000).
[12] T. Waas, N. Kaiser and W. Weise, Phys. Lett. B **379**, 34 (1996).
[13] W. Cassing, E. L. Bratkovskaya, U. Mosel, S. Teis and A. Sibirtsev, Nucl. Phys. A **614**, 415 (1997).
[14] T. Waas, M. Rho and W. Weise, Nucl. Phys. A **617**, 449 (1997).
[15] G. Q. Li, C.-H. Lee and G. E. Brown, Nucl. Phys. A **625**, 372 (1997).
[16] Z. S. Wang, A. Faessler, C. Fuchs, V. S. U. Maheswari and T. Waindzoch, Phys. Rev. C **57**, 3284 (1998).
[17] G. Q. Li and G. E. Brown, Phys. Rev. C **58**, 1698 (1998).
[18] E. L. Bratkovskaya, W. Cassing and U. Mosel, Phys. Lett. B **424**, 244 (1998).
[19] W. Cassing and E. L. Bratkovskaya, Phys. Rep. **308**, 65 (1999).
[20] C. Hartnack, H. Oeschler and J. Aichelin, nucl-th/0109016.
[21] J. Aichelin and C. Hartnack, J. Phys. G **27**, 571 (2001).
[22] N. Herrmann for the FOPI collaboration, Nucl. Phys. A **610**, 49c (1996).
[23] R. Kotte for the FOPI Collaboration, Proceedings of HIRSCHEGG2000, HADRONS IN DENSE MATTER, International Workshop XXVIII on Gross Properties of Nuclei and Nuclear Excitations, Hirschegg, Austria, Jan 16-22, 2000, edited by M. Buballa, W. Nörenberg, B.-J. Schäfer, J. Wambach, p. 112
[24] R. Kotte, A. Mangiarotti, N. Herrmann et al. (FOPI collaboration), to be published.
[25] A. Sibirtsev, W. Cassing and C. M. Ko, Z. Phys. A **358**, 101 (1997).
[26] W. S. Chung, G. Q. Li and C. M. Ko, Phys. Lett. B **401**, 1 (1997).
[27] W. S. Chung, G. Q. Li and C. M. Ko, Nucl. Phys. A **625**, 347 (1997).
[28] W. S. Chung, C. M. Ko and G. Q. Li, Nucl. Phys. A **641**, 357 (1998).
[29] A. I. Titov, B. Kämpfer, V. V. Shklyar, Phys. Rev. C **59**, 999 (1999).
[30] K. Nagayama, J. W. Durso, J. Haidenbauer, C. Hanhart, J. Speth, Phys. Rev. C **60**, 055209 (1999).
[31] A. I. Titov, B. Kämpfer and B. L. Reznik, Eur. Phys. J. A **7**, 543 (2000).
[32] H. W. Barz and B. Kämpfer, Nucl. Phys. A **683**, 594 (2001).
[33] H. W. Barz, M. Zétényi, Gy. Wolf and B. Kämpfer, nucl-th/0110013; Nucl. Phys. A, in press.
[34] F. Balestra et al. (DISTO collaboration), Phys. Rev. Lett. **81**, 4572 (1998); Phys. Lett. B **468**, 7 (1999); Phys. Rev. C **63**, 024004 (2001).
[35] M. Büscher et al. (ANKE collaboration), COSY proposal #104.
[36] C. Hartnack and J. Aichelin, private communication.
[37] F. Klingl, T. Waas and W. Weise, Phys. Lett. B **431**, 254 (1998); F. Klingl, N. Kaiser and W. Weise, Nucl. Phys. A **624**, 527 (1997).
[38] E. Oset and A. Ramos, Nucl. Phys. A **679**, 616 (2001).
[39] J. Friese for the HADES collaboration, Nucl. Phys. A **654**, 1017c (1999); Progr. in Part. and Nucl. Phys. **42**, 235 (1999); C. Garabatos for the HADES collaboration, Nucl. Phys. B **61**, 607 (1998); web site: http://www-hades.gsi.de/.
[40] A. Gobbi et al. (FOPI collaboration), Nucl. Instr. Meth. A **324**, 156 (1993); J. Ritman for the FOPI collaboration, Nucl. Phys. (Proc. Suppl.) B **44**, 708 (1995); web site: http://www-

aix.gsi.de/~fopiwww/
[41] C. Finck for the FOPI collaboration, XXXIX INTERNATIONAL WINTER MEETING ON NUCLEAR PHYSICS, Bormio, Italy, Jan 22-27, 2001, Ricerca Scientifica ed Educazione Permanente Supplemento, Edited by I. Iori; web site: http://www-aix.gsi.de/~fopiwww/npro/
[42] Particle Data Group, Eur. Phys. J. A **3**, 376 (1998).
[43] S. A. Bass, C. Hartnack, H. Stöcker and W. Greiner, Phys. Rev. C **51**, 3343 (1995); C. Hartnack, Rajeev K. Puri, J. Aichelin, J. Konopka, S. A. Bass, H. Stöcker, W. Greiner, Eur. Phys. J. A **1**, 151 (1998).
[44] P. J. Siemens and J. O. Rasmussen, Phys. Rev. Lett. **42**, 880 (1979).
[45] W. Reisdorf et al. (FOPI collaboration), Nucl. Phys. A **612**, 493 (1997).
[46] D. Best et al. (FOPI collaboration), Nucl. Phys. A **625**, 307 (1997).
[47] B. Hong et al. (FOPI collaboration), Phys. Rev. C **57**, 244 (1998); Phys. Rev. C **58**, 603 (1998).
[48] B. Holzman for the E917 collaboration, nucl-ex/0103015.
[49] L. Ahle et al. (E866, E917 collaboration), Phys. Lett. B **490**, 53 (2000).
[50] W. Cassing, E. Bratkovskaya and S. Juchem, Nucl. Phys. A **674**, 249 (2000).
[51] "Dilepton Production in CC and $\pi^{\pm}p$ Reactions", HADES beamtime proposal, May 18th, 2001, http://www-hades.gsi.de/.

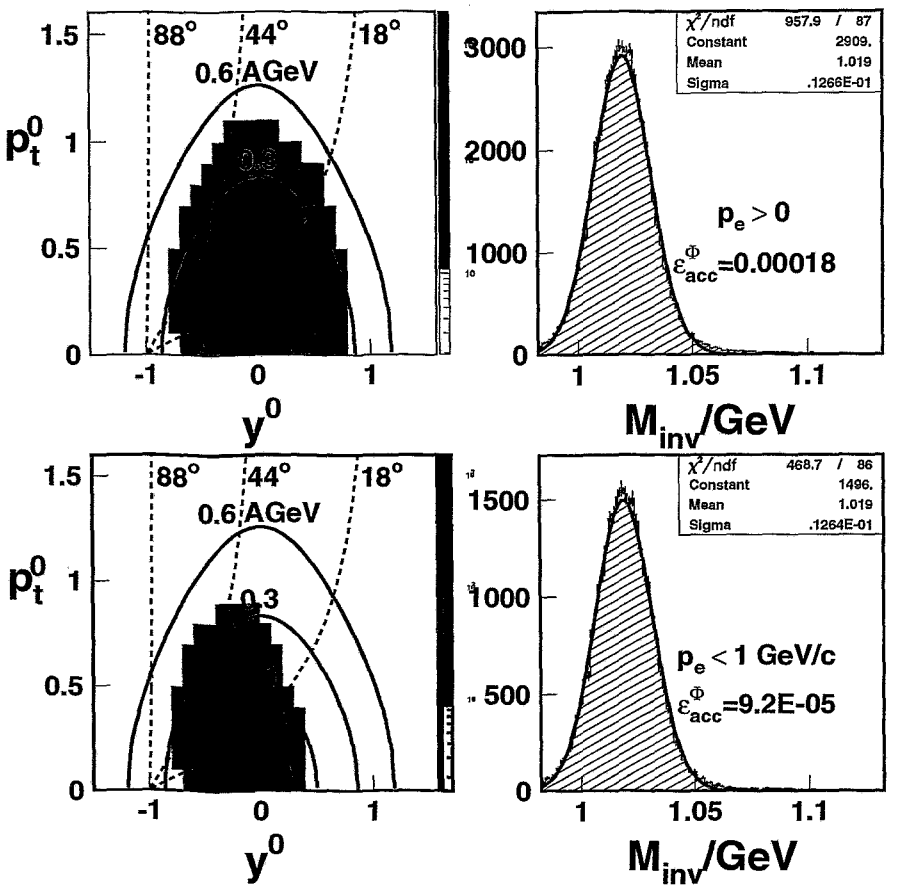

FIG. 1. Left panels: Monte-Carlo simulation of the two-dimensional distribution of yields $d^2N/dp_t dy$ of ϕ mesons in the $p_t^0 - y^0$ plane reconstructed from pairs of electrons and positrons which are accepted within the polar angle range of $18^o < \theta_e < 88^o$. The mother ϕ's are generated by means of an isotropic thermal model with inverse slope parameter $T_\phi = 70$ MeV. Here, $p_t^0 = (p_t/A)/(p_{proj}/A_{proj})_{cm} = (\beta_t\gamma)/(\beta\gamma)_{cm}^{proj}$ and $y^0 = (y/y_{proj})_{cm} = (y/y_{cm} - 1)$ are the normalized transverse momentum and rapidity, respectively, and $A = m/m_p$ is the particle mass number. Both observables are related to the corresponding projectile quantities in the center-of-mass (c.m.) frame of the colliding nuclei (with $y_{cm} = 0.904$ and $(\beta\gamma)_{cm}^{proj} = 1.032$ for 2 A·GeV beam energy). The dashed (full) lines represent constant polar angles in the laboratory (constant kinetic energies per nucleon in the c.m. system). A logarithmic intensity scale is used. Right panels: The corresponding invariant mass distributions reconstructed from correlated e^+e^- pairs. The electron momentum regions and the calculated acceptance factors (including the branching ratio $\frac{\Gamma_{\phi\to e^+e^-}}{\Gamma_{\phi,tot}} = 3 \cdot 10^{-4}$) are indicated. The full lines display Gaussian fits with the resulting mean values and sigma widths given in the inserts in the upper right corners. A relative momentum resolution of $\delta p/p = 0.015$ is assumed.

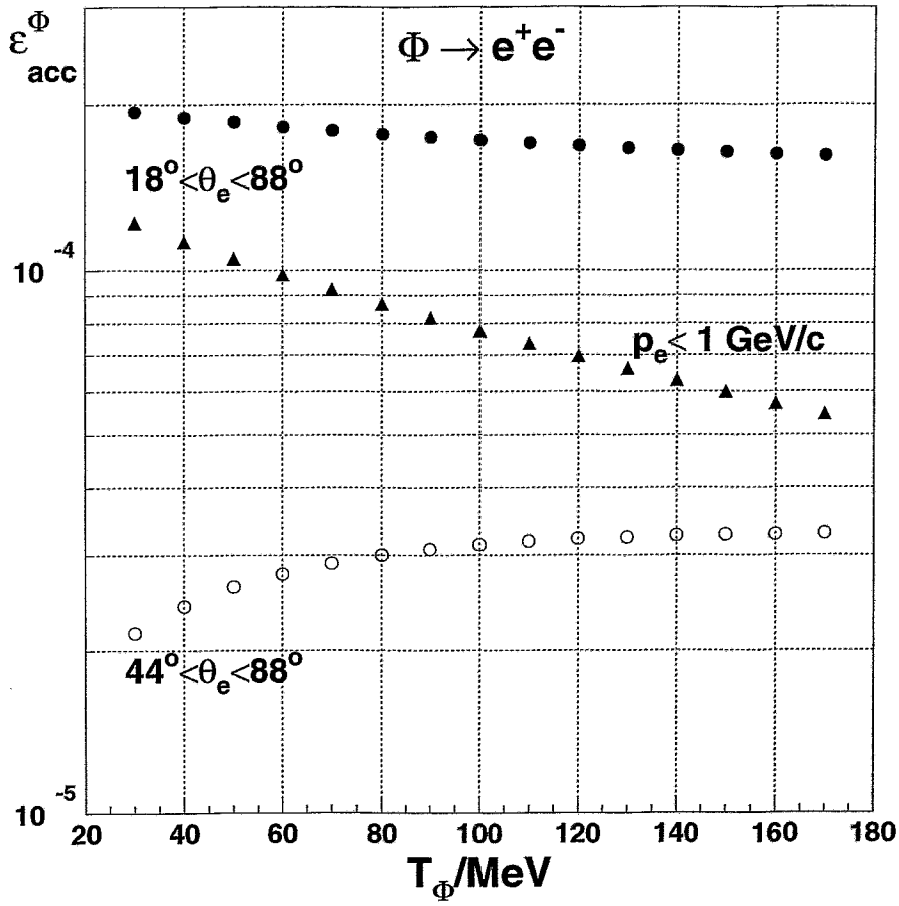

FIG. 2. The acceptance factor (including the branching ratio $\frac{\Gamma_{\phi \rightarrow e^+e^-}}{\Gamma_{\phi,tot}} = 3 \cdot 10^{-4}$) of the detection of correlated e^+e^- pairs within HADES vs. the inverse slope parameter T of the mother ϕ mesons generated within an isotropic thermal model. Full (open) symbols are for a minimum polar angle of the electrons/positrons of 18 (44) degrees, respectively. Triangles represent the output of the Monte-Carlo simulation when accepting only leptons with momenta smaller than 1 GeV/c.

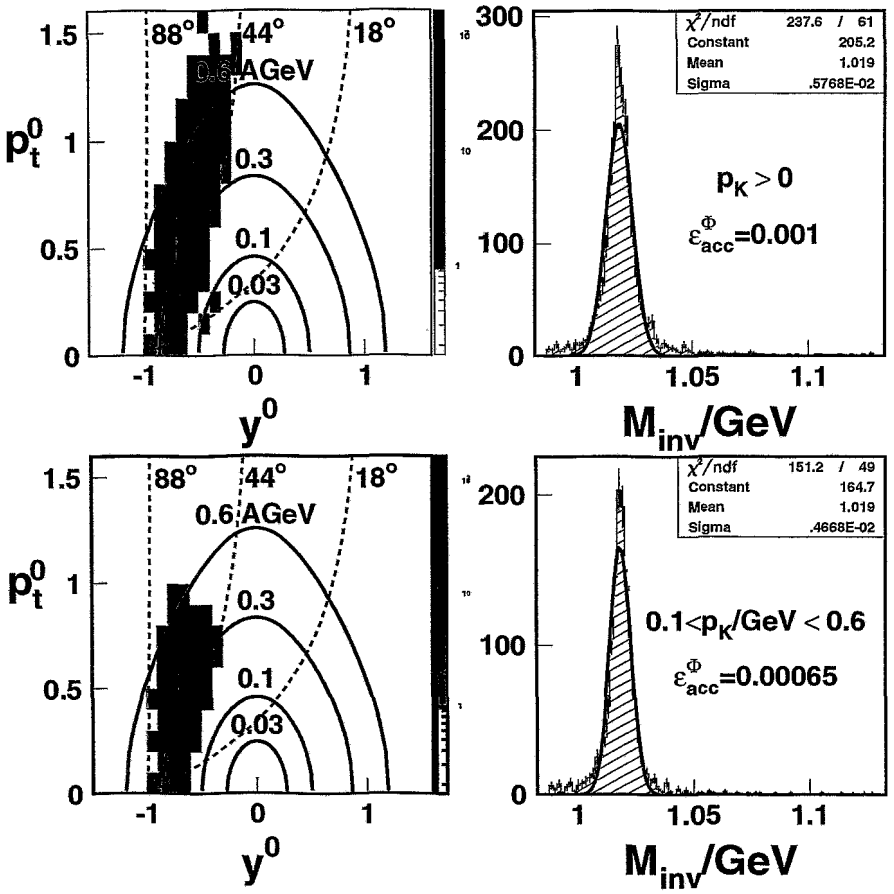

FIG. 3. The same as fig. 1 but for the decay channel $\phi \rightarrow K^+K^-$ to be measured within the present HADES acceptance region with high TOF resolution and sufficient granularity allowing for kaon identification over the polar angle range of $44^o < \theta_K < 88^o$. No $K^{\pm}$ momentum cuts are applied for the ϕ phase-space (left) and invariant mass distributions (right) given in the upper panels. The lower panels show the corresponding results when selecting kaons with momenta of 0.1 GeV/c $< p_K <$ 0.6 GeV/c.

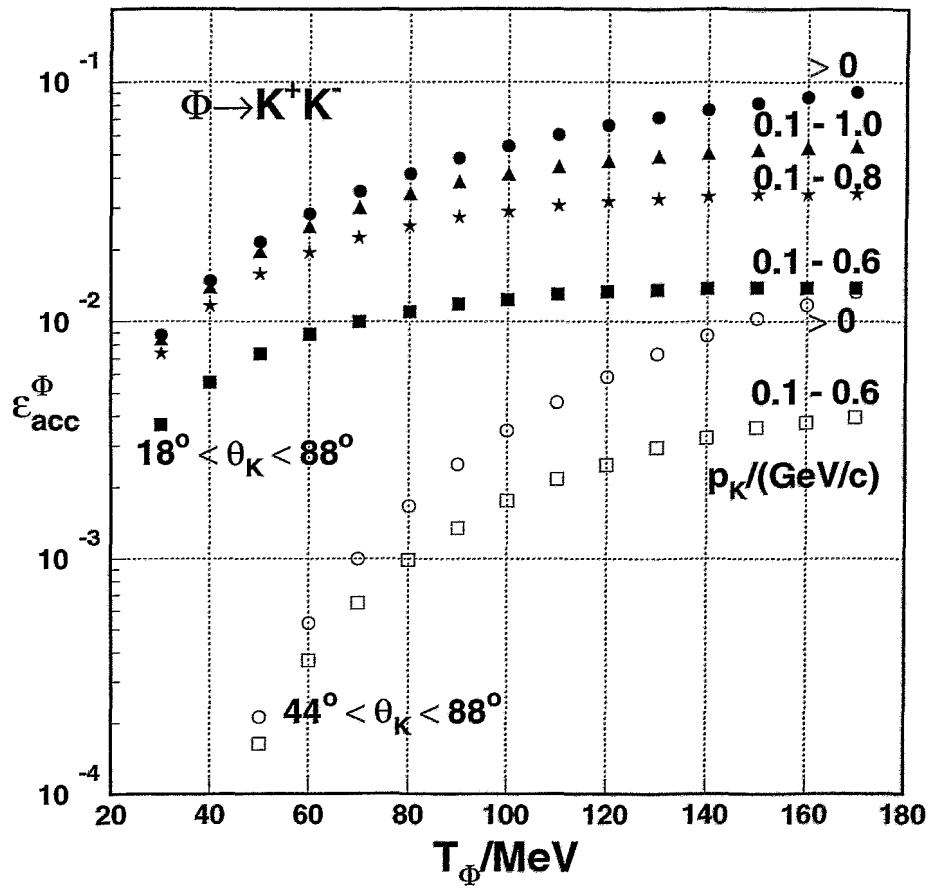

FIG. 4. The same as fig. 2 but for the hadronic decay channel $\phi \rightarrow K^+K^-$ to be measured with HADES(including the branching ratio $\frac{\Gamma_{\phi\rightarrow K^+K^-}}{\Gamma_{\phi,tot}} = 0.492$). Full (open) symbols represent the output of the simulation for a lower $K^{\pm}$ polar angle of 18 (44) degrees. Dots give the results of the Monte-Carlo simulation without momentum restriction. Triangles, stares and squares show the acceptance factor if only kaons/antikaons with minimum momentum of 0.1 GeV/c and maximum momentum of 1 GeV/c, 0.8 GeV/c and 0.6 GeV/c are accepted, respectively.

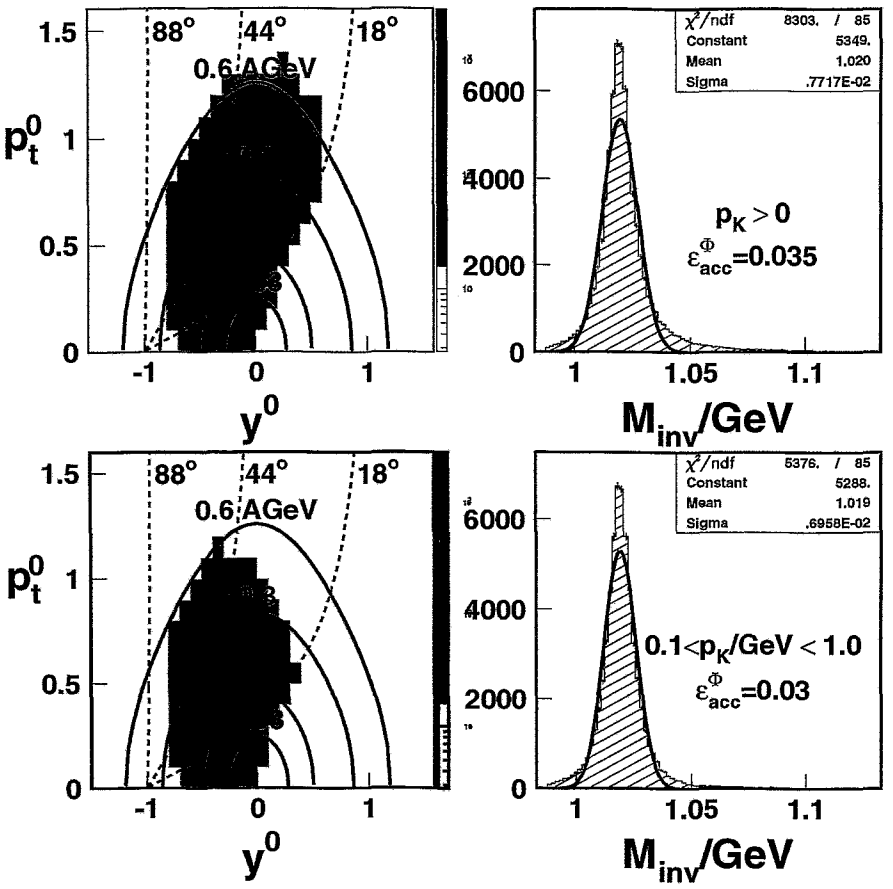

FIG. 5. The same as fig. 3 but for a possible upgrade of the HADES-TOF detector allowing for kaon identification over the polar angle range of $18^o < \theta_K < 88^o$. No kaon momentum cuts are applied for the ϕ phase-space (left) and invariant mass distributions (right) given in the upper panels. The lower panels show the corresponding results when selecting kaons with momenta of 0.1 GeV/c $< p_K <$ 1.0 GeV/c.

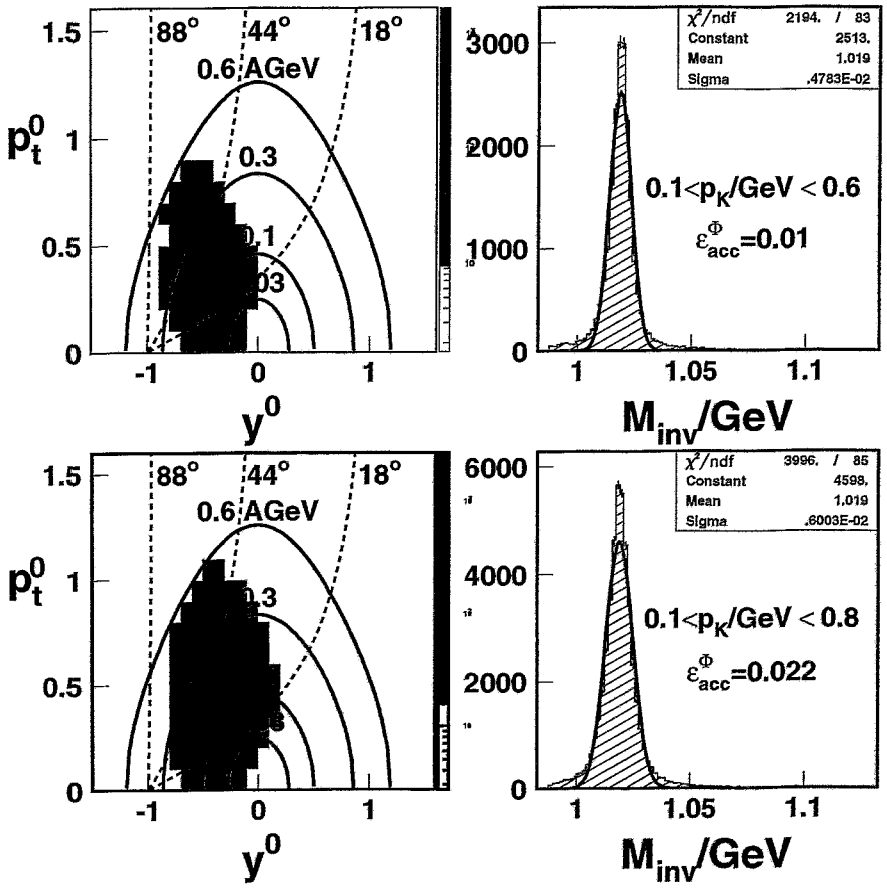

FIG. 6. The same as fig. 5 but for a maximum momentum of the $K^{\pm}$ mesons of 0.6 GeV/c (upper panels) and 0.8 GeV/c (lower panels).

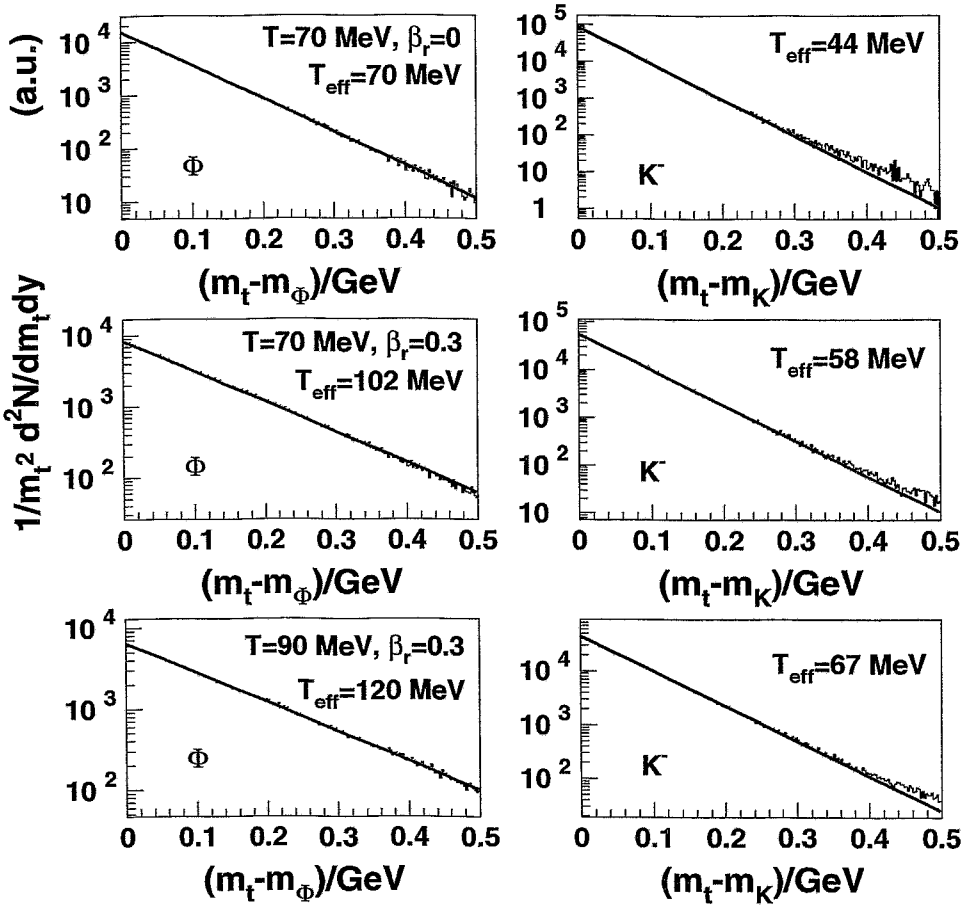

FIG. 7. The transverse mass distribution at midrapidity (eq. (1), $|y^0| < 0.2$) of the ϕ mesons (left panels) and the antikaons from their decay (right panels) for different combinations of the temperature and flow velocity parameters. Solid lines represent fits to the spectra with a single exponential function. The resulting effective inverse slope parameters T_{eff} are given in the panels. Note the steeper slope of the daughter $K^{\pm}$ mesons as a result of the ϕ decay kinematics.

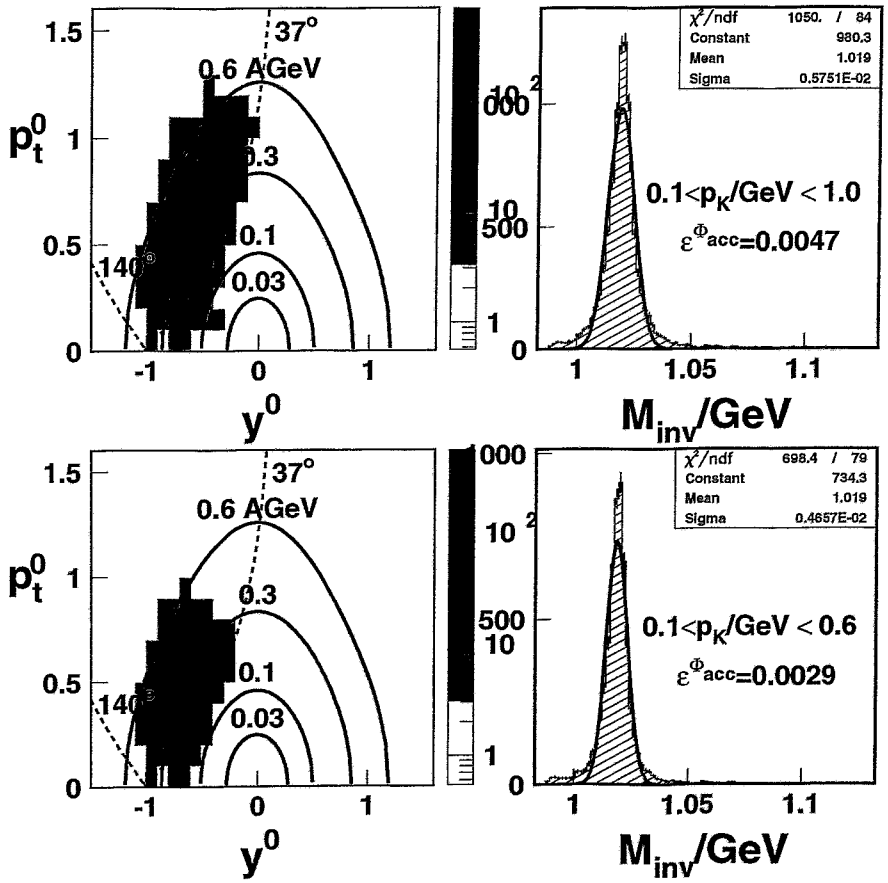

FIG. 8. The same as fig. 1 but for the decay channel $\phi \rightarrow K^+K^-$ to be measured with the FOPI detector combination of CDC and upgraded TOF barrel. Here, the lower and upper polar angle limits are 37 and 140 degrees, respectively. In the upper panels a maximum $K^{\pm}$ momentum of 1 GeV/c is assumed as expected for the upgraded TOF barrel version. The lower panels show the results of the simulation when applying the upper limit necessary for ϕ identification with the present TOF barrel version and the CDC.

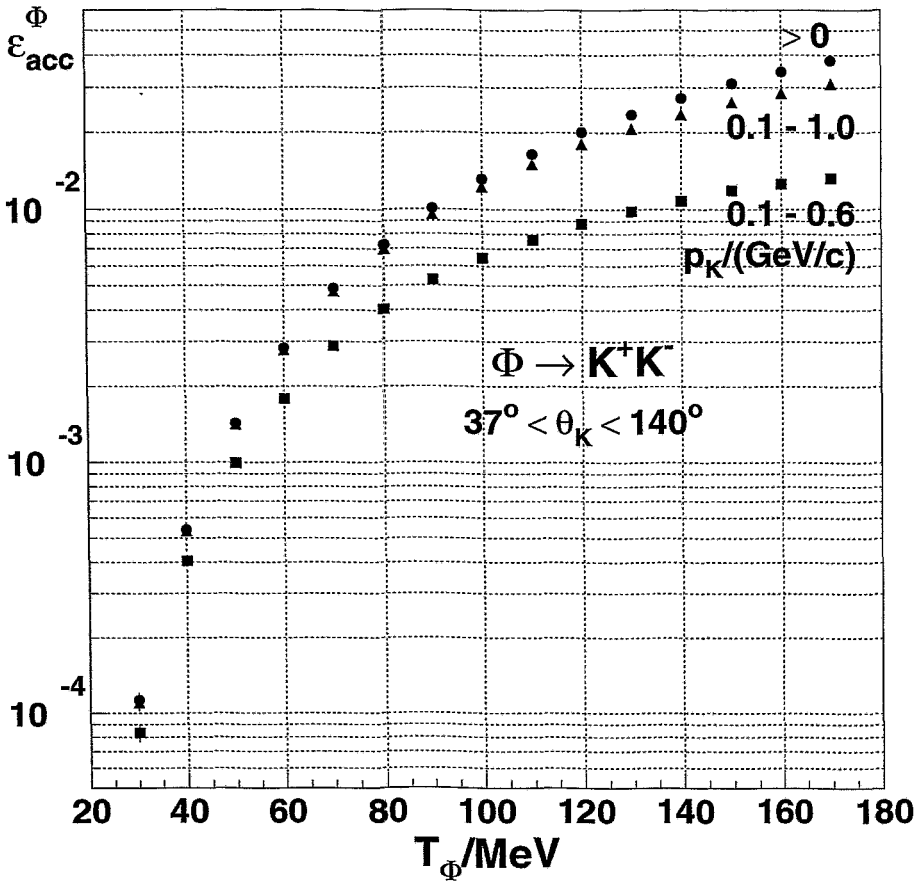

FIG. 9. The same as fig. 2 but for the hadronic decay channel $\phi \rightarrow K^+K^-$ (including the branching ratio $\frac{\Gamma_{\phi \rightarrow K^+K^-}}{\Gamma_{\phi,tot}} = 0.492$) to be measured with the FOPI detector combination of CDC and upgraded TOF barrel. Here, the lower and upper polar angle limits are 37 and 140 degrees, respectively. The investigated kaon momentum ranges are indicated.

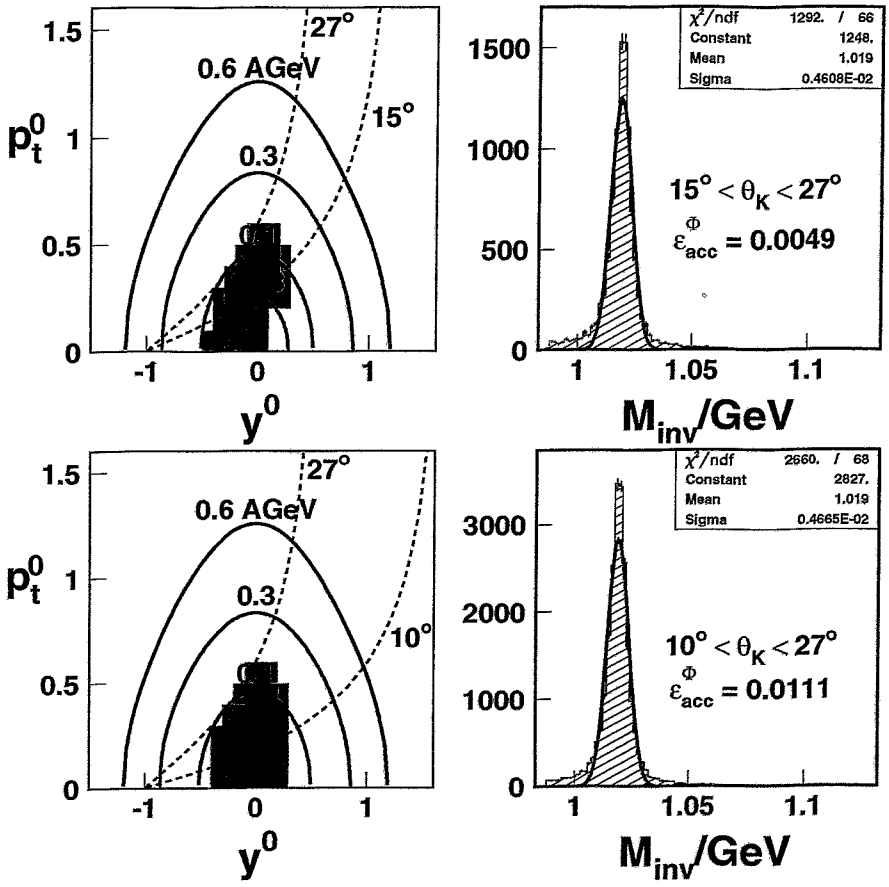

FIG. 10. The same as fig. 8 but for the FOPI detector combination of Helitron and Plastic Wall. Here, the kaon velocity is restricted to $0.4 < \beta_K < 0.85$. The maximum polar angle amounts to 27 degrees. The lower and upper panels give the results of the simulation for minimum $K^{\pm}$ polar angles of 10 and 15 degrees, respectively. A time resolution of 200 ps is taken into account.

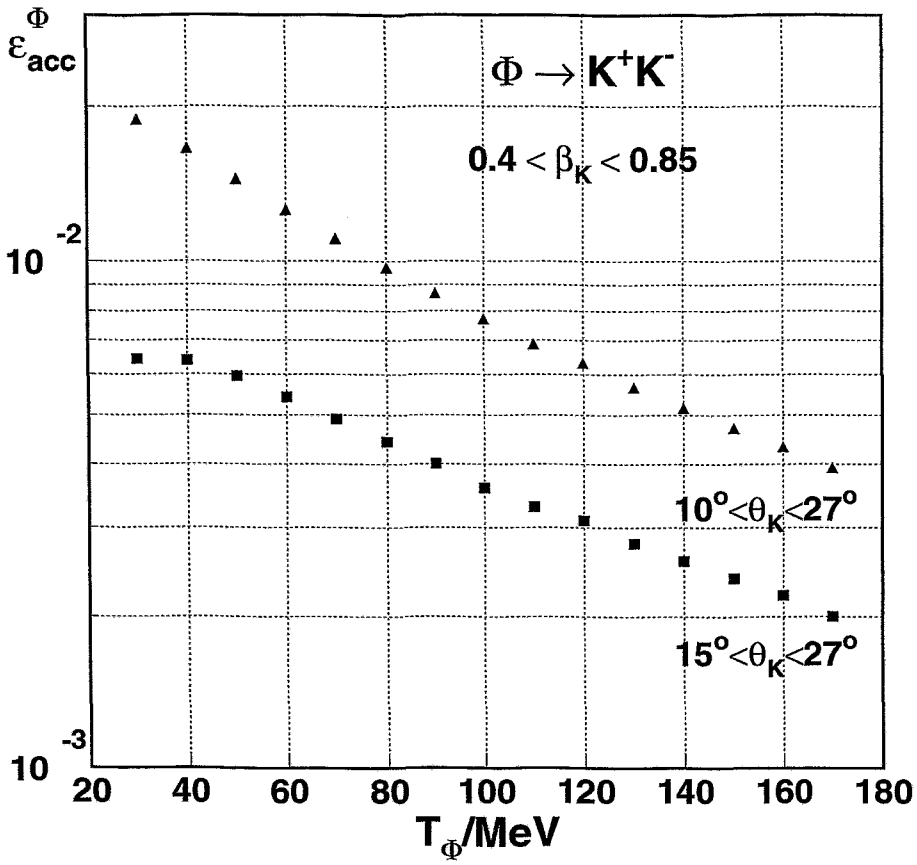

FIG. 11. The same as fig. 9 but for the phase-space region accessible with the Helitron/Plastic Wall combination of the FOPI detector system. The investigated kaon velocity and polar angle limits are indicated.

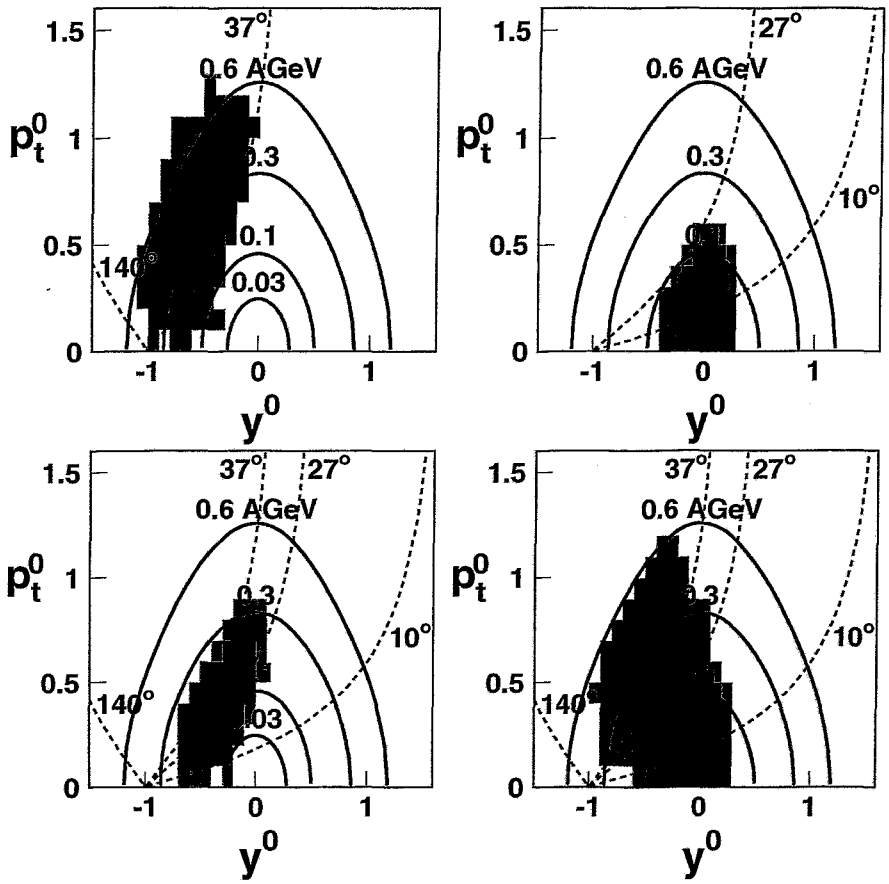

FIG. 12. The phase-space distributions of ϕ mesons to be measured with different detector combinations of the FOPI setup. Upper left panel: CDC with upgraded TOF barrel (0.1 GeV/c $< p_K <$ 1 GeV/c); upper right panel: Hel/Pla ($0.4 < \beta_K < 0.85$); lower left panel: mixed yield when detecting K^+ mesons in Hel/Pla and K^- mesons in CDC/Bar; lower right panel: sum of the other three distributions. Dashed lines display the polar angle limits for kaon detection of the corresponding subdetectors.

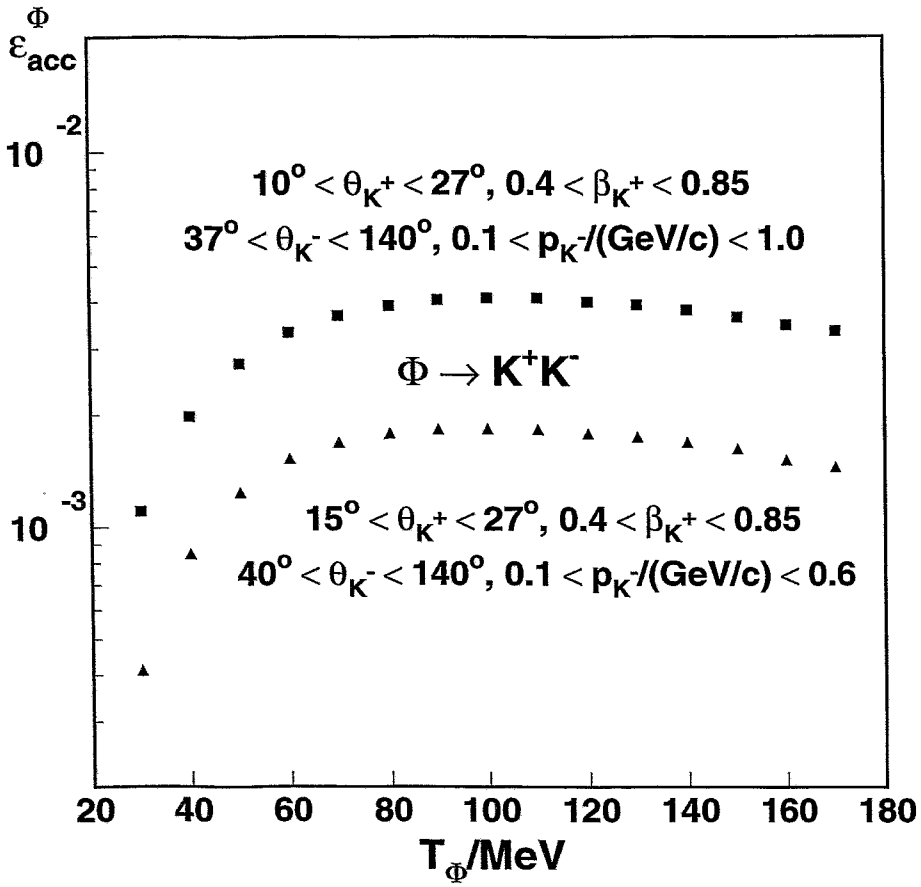

FIG. 13. The same as fig. 9 but for detecting the K^+ mesons in the FOPI subdetectors Helitron and Plastic Wall whereas the K^- mesons are identified by the CDC and the upgraded TOF barrel. The investigated kaon velocity and polar angle limits are indicated.